Methyl halides in surface seawater and marine boundary layer of the northwest Pacific

Atsushi Ooki,[1] Atsushi Tsuda,[2] Sohiko Kameyama,[1,3] Shigenobu Takeda,[4,5] Sachihiko Itoh,[2] Toshio Suga,[6,7] Hirofumi Tazoe,[8] Ayako Okubo,[2,9] and Yoko Yokouchi[1]

Received 7 August 2009; revised 6 April 2010; accepted 10 June 2010; published 8 October 2010.

[1] The partial pressures of methyl halides (CH_3X; X = Cl, Br, or I) and of $CHClF_2$ (HCFC-22), which are all volatile organic compounds (VOCs), were measured in the air of the marine boundary layer ($pVOC_{air}$) and in surface seawater ($pVOC_{water}$) during a cruise from the subarctic to subtropical regions of the northwest Pacific in summer of 2008. In the northern transition water (TW_N) with high biological activity, high levels of the three CH_3Xs in surface seawater were frequently observed, probably owing to their enhanced production by phytoplankton. Supersaturation of CH_3Br was only present in TW_N water, with a saturation anomaly (SCH_3Br) of 0.95 [$SCH_3X = (pCH_3X_{water} - pCH_3X_{air})/pCH_3X_{air}$]. The highest saturation anomalies for CH_3Cl (SCH_3Cl = 1.6) and CH_3I (SCH_3I = 91) were found in the southern subtropical water (ST_S) with low biological production south of the subtropical front. We found that the molar concentrations of CH_3Cl (CCH_3Cl) and CH_3I (CCH_3I) sharply increased with increasing sea surface temperature (SST) in the subtropical waters. The maximum CCH_3Cl (144 pmol l^{-1}) was present in ST_S water at SST = 30°C and is 1.5 times the value extrapolated from the previously reported relationship between CCH_3Cl and SST. Photochemical production might have contributed to the production of CH_3Cl and CH_3I in ST_S water.

Citation: Ooki, A., A. Tsuda, S. Kameyama, S. Takeda, S. Itoh, T. Suga, H. Tazoe, A. Okubo, and Y. Yokouchi (2010), Methyl halides in surface seawater and marine boundary layer of the northwest Pacific, *J. Geophys. Res.*, *115*, C10013, doi:10.1029/2009JC005703.

1. Introduction

[2] Methyl chloride (CH_3Cl) and methyl bromide (CH_3Br) have been regarded as the largest contributors of naturally produced halogens to the stratosphere, where they are responsible for ozone destruction [*World Meteorological Organization* (*WMO*), 2007], while methyl iodide (CH_3I) primarily affects ozone destruction in the troposphere [*Chameides and Davis*, 1980] and in the lower stratosphere [*Solomon et al.*, 1994].

[3] A number of studies have investigated the oceanic sources and sinks of methyl halides (CH_3X). Biological sources include macroalgae [*Manley and Dastoor*, 1987; *Manley*, 1992; *Giese et al.*, 1999], phytoplankton [*Scarratt and Moore*, 1996; *Manley and dela Cuesta*, 1997; *Scarratt and Moore*, 1998], and bacteria for CH_3I [*Amachi et al.*, 2001; *Smythe-Wright et al.*, 2006]. Bacterial degradation of CH_3Cl and CH_3Br is reportedly an important oceanic sink for these molecules [*Tokarczyk et al.*, 2003a, 2003b]. Abiotic processes involving methyl halides include nucleophilic substitution of CH_3Br and CH_3I by Cl^- (chloride substitution), resulting in CH_3Cl [*Elliott and Rowland*, 1993; *Jones and Carpenter*, 2007], as well as photochemical production of CH_3I from I and methyl radicals [*Moore and Zafiriou*, 1994; *Happell and Wallace*, 1996; *Yokouchi et al.*, 2001, 2008; *Richter and Wallace*, 2004; *Chuck et al.*, 2005] and CH_3Cl from colored dissolved organic compounds (CDOM) [*Moore*, 2008].

[4] To estimate the global oceanic distributions of methyl halides and their oceanic fluxes, several studies examined correlations between CH_3X concentrations and key oceanic parameters such as sea surface temperature (SST). The relationships between SST and concentrations of CH_3Cl and CH_3Br were used to estimate global oceanic fluxes, by extrapolation from the global SST distribution, for CH_3Cl

[1]National Institute for Environmental Studies, Ibaraki, Japan.
[2]Atmosphere and Ocean Research Institute, University of Tokyo, Tokyo, Japan.
[3]Now at Faculty of Environmental Earth Science, Hokkaido University, Hokkaido, Japan.
[4]Graduate School of Agricultural and Life Sciences, University of Tokyo, Tokyo, Japan.
[5]Also at Faculty of Fisheries, Nagasaki University, Nagasaki, Japan.
[6]Department of Geophysics, Graduate School of Science, Tohoku University, Miyagi, Japan.
[7]Also at Institute of Observational Research for Global Change, Japan Agency for Marine Earth Science and Technology, Kanagawa, Japan.
[8]College of Humanities and Sciences, Nihon University, Tokyo, Japan.
[9]Now at Graduate School of Agricultural and Life Sciences, University of Tokyo, Tokyo, Japan.

0148-0227/10/2009JC005703

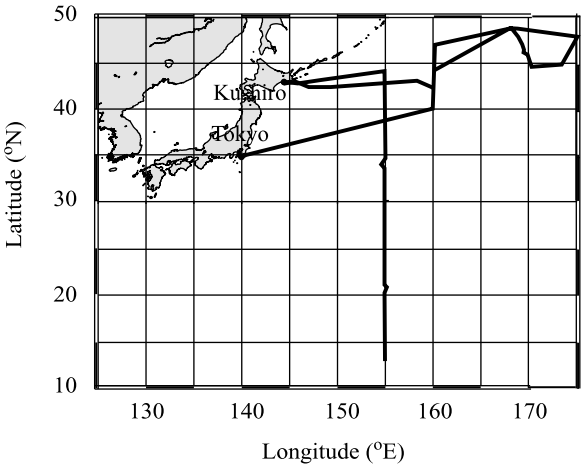

Figure 1. Track of R/V *Hakuho* cruise KH08-2 in 2008.

(0.3−0.7 Tg y^{-1}) [*Khalil et al.*, 1999; *Moore*, 2000; *Yoshida et al.*, 2004] and for CH_3Br (−10 to −21 Gg y^{-1}) [*Lobert et al.*, 1995; *Groszko and Moore*, 1998]. *Bell et al.* [2002] estimated the global oceanic flux of CH_3I (0.2 Tg y^{-1}) by integrating the photochemical production of CH_3I as a function of solar radiation and dissolved organic carbon concentration. *Butler et al.* [2007] reported the average CH_3I flux in major oceanic waters, tropical, subtropical, temperate, polar, subpolar, and coastal, and extrapolated the results to obtain the global oceanic flux of 0.6 Tg y^{-1}. On the basis of these flux estimates, the ocean is considered to be the second largest source of CH_3Cl, and the second largest net sink of CH_3Br, and a major source of CH_3I. It is expected that the fluxes, such as the ones given above, will be altered by climate change influences on the air-sea flux of CH_3X caused by a rise in SST and other changes in marine ecosystems [*Anbar et al.*, 1996; *Smythe-Wright et al.*, 2006; *Butler et al.*, 2007]. For quantitative predictions of changes in CH_3X flux, it is therefore essential to understand the mechanisms of production and loss of CH_3X in seawater.

[5] For understanding the CH_3X variability in surface seawater associated with mesoscale water mass structure, CH_3X concentrations need to be determined with high frequency at a measurement cycle of several hours intervals on a ship which corresponds to several tens kilometers intervals. Recently, high-frequency measurements of CH_3I and brominated halocarbons have been carried out in surface seawater and air in the Atlantic and East Pacific by means of a liquid-gas equilibrator and gas chromatograph-mass spectrometer (GC-MS) system [*Butler et al.*, 2007]. However, there have been no high-frequency measurement studies of the 3 CH_3Xs in the NW Pacific, including the subarctic water and mixed water (subarctic-subtropical transition zone) with well-known high primary production, and the oligotrophic subtropical region, which has the warmest SST, of up to 30°C in summer. To characterize the oceanic distributions of CH_3Xs in the NW Pacific, we measured 3 CH_3Xs (CH_3Cl, CH_3Br and CH_3I) and HCFC-22 in surface seawater and in the marine boundary layer (MBL) of the NW Pacific from subarctic to subtropical regions by means of a liquid-gas equilibrator and GC-MS system as a part of the Japanese Surface Ocean Lower Atmosphere Study (J-SOLAS). HCFC-22 is long-lived in air with lifetime of 12.0 years [*WMO*, 2007] and is derived from terrestrial anthropogenic sources. Because it is mainly affected by physical processes such as air-sea exchange, temperature-dependent solubility and mixing, it was investigated as an indicator of the behavior of a dissolved gas that is not affected by chemical or biological processes.

2. Methods

2.1. VOC Measurements

[6] VOC measurements were conducted aboard the R/V *Hakuho-maru* (cruise KH08-2) in 2008 from 29 July to 19 August (Leg 1) and from 23 August to 15 September (Leg 2) in the NW Pacific (Figure 1). Surface seawater was pumped from a seawater intake on the bottom of the ship (5 m depth), and supplied to the laboratory, passing through a seawater pipe with the inner wall coated with nylon for most of its length. The surface seawater was continuously supplied to a silicone membrane tube equilibrator at a flow rate of 15 L min^{-1}. Details of CH_3X measurements are described elsewhere [*Ooki and Yokouchi*, 2008]. Briefly, the equilibrator consists of six silicone tubes (length, 10 m; o.d., 2.0 mm; i.d., 1.5 mm) housed in a polyvinyl chloride (PVC) pipe. Pure air was continuously supplied to the silicone tubes at a flow rate of 25 mL min^{-1}, regulating the inner pressure to +0.14 MPa. The gas-phase sample of VOCs at equilibrium with the seawater could be obtained from the outlet of the silicone tube. The equilibrator was cleaned by compressed air to remove deposits after Leg 1.

[7] Outside air was drawn from the upper deck (17 m above the sea level) of the ship through a PTFE tube (length, 60 m; i.d., 11 mm) at a flow rate of 50 L min^{-1}. We obtained a portion of the air from the PTFE tube at a flow rate of 25 mL min^{-1} using a metal bellows pump. The gas phase sample (equilibrated air or outside air) was dehumidified by means of Nafion® dryer and then transferred to a preconcentration/GC-MS system [*Yokouchi et al.*, 2006]. Partial pressures of CH_3Cl, CH_3Br, CH_3I, and HCFC-22 in the sample of equilibrated air or outside air were measured at 70 min intervals. A gravimetrically prepared standard gas (Taiyo Nissan, Inc., Tokyo) containing these chemical species at concentrations of 100–500 pptv was quantified according to the same procedures. The detection limits (S/N = 3) were 0.1–1 pptv for all species. The analytical precisions of *p*VOC for all the species based on the repetitive analyses of standard gas were within 1%. Overall precisions for the seawater samples were also evaluated on the basis of the observation results at the fixed sampling location (N20°, E155°) for the duration of 2 days during the cruise. The overall precisions of $pVOC_{water}$ (n = 38) were 3.6% for CH_3Cl, 6.9% for CH_3Br, 2.9% for CH_3I, and 1.3% for HCFC-22. To be noted that these overall precisions suffer from their natural variability in addition to the measurement errors.

2.2. Sampling Line Artifact Test

[8] To test for possible contamination or loss of CH_3X in the ship's seawater sampling line, we also used a separate, brand-new sampling line including seawater intake, pump, pipe and equilibrator to collect surface seawater in parallel

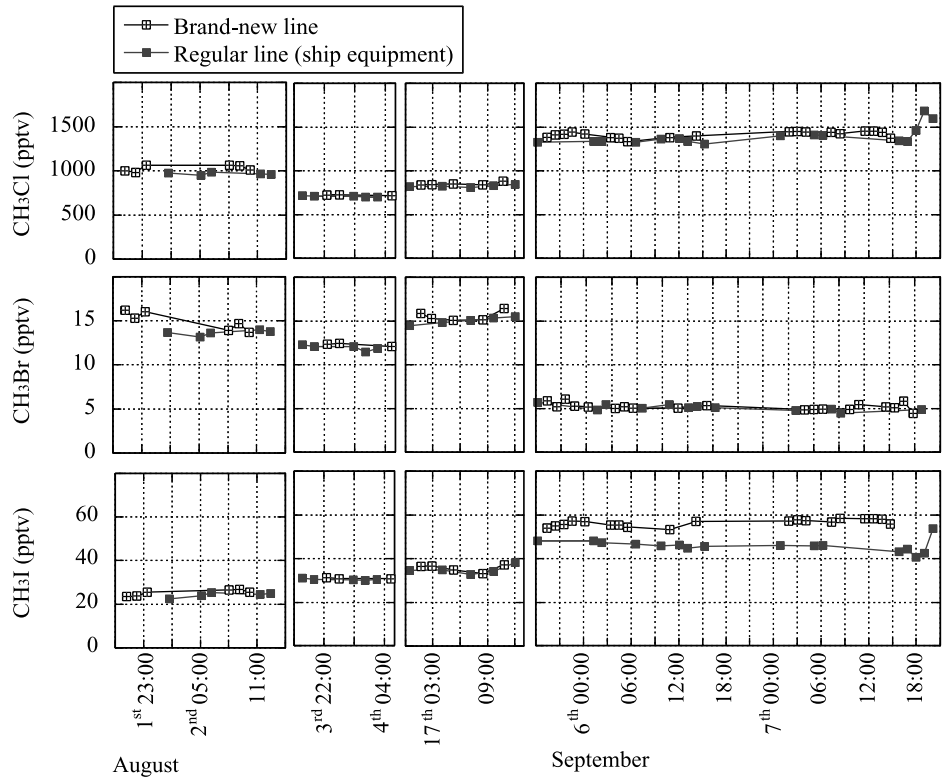

Figure 2. Seawater sampling line artifact test.

with the ship's regular sampling system. The surface seawater was drawn in by a stainless-steel screw pump through a fluororesin tube (length, 10 m; i.d., 12 mm), and transferred to the brand-new equilibrator through a Tygon® tube (length, 20 m; i.d., 13 mm). VOCs would permeate through the Tygon tube to some extent. To minimize the influence of VOCs permeation, surface seawater flowed over 3 h before the sampling line artifact test. The residence time of seawater in the Tygon tube was about 15 s. We considered that contaminations and losses of CH_3X in the brand-new sampling line are negligible. Comparisons were done at 4 different times, 3 times during leg 1 and once during leg 2.

2.3. Chlorophyll-a Measurement

[9] Some of the environmental parameters (salinity, temperature, and chlorophyll-a) were continuously monitored with an AMEMBO II, which was a modified version of the AMEMBO system [*Tsuda et al.*, 1993]. The system consisted of a bubble trap, thermosalinograph (SeaBird SBE21) and in vivo chlorophyll fluorometer (Wetlab). Seawater was pumped up to the system from the bottom of the ship. The chlorophyll-a concentrations determined by the AMEMBO II were calibrated against those of 107 extracted chlorophyll-a from filter samples, which were measured on board using a Turner Designs fluorometer [*Welschmeyer*, 1994].

3. Results

3.1. Sampling Line Artifact

[10] We found that for CH_3Cl and CH_3Br, there were no significant differences in their partial pressures when the sampling lines were switched (Figure 2). This result suggests that contamination and loss of these compounds in the sampling lines were negligible. As for CH_3I, the partial pressure was consistently lower by about 12% when the sampling line was switched from the "brand new" line to the "regular" line during the second leg. This indicates that about 12% of CH_3I in seawater was lost in the regular line during the second leg. This methyl iodide might have been lost through interaction with the iron mold-like deposits that were found on the inner surface of the equilibrator. We applied a 12% correction to the measured pCH_3I in the surface seawater during the second leg under the assumption that the constant rate (12%) of the CH_3I had been lost.

3.2. Water Type and Chlorophyll-a Concentration

[11] The frontal structure in the subarctic-subtropical transition area in NW Pacific is characterized by the cold Oyashio current and the warm Kuroshio current [*Yasuda*, 2003]. From the conductivity-temperature-depth (CTD) profiles obtained at intervals of 1° along 155°E from 44°N to 12°N, we identified the subarctic front, the subarctic boundary, the Kuroshio extension front, and the subtropical front at around 44°N, 40°N, 32°N, and 25°N, respectively (Figure 3). Latitudinal distributions of SST and chlorophyll-a concentration in surface seawater are shown in Figure 3. We classified the surface seawater into five water types: (1) subarctic water (SA) to the north of the subarctic front in 44–49°N (approximately SST = 11–16°C); (2) northern transition water (TW_N) between the subarctic front and the subarctic boundary in 40–44°N (approximately SST =

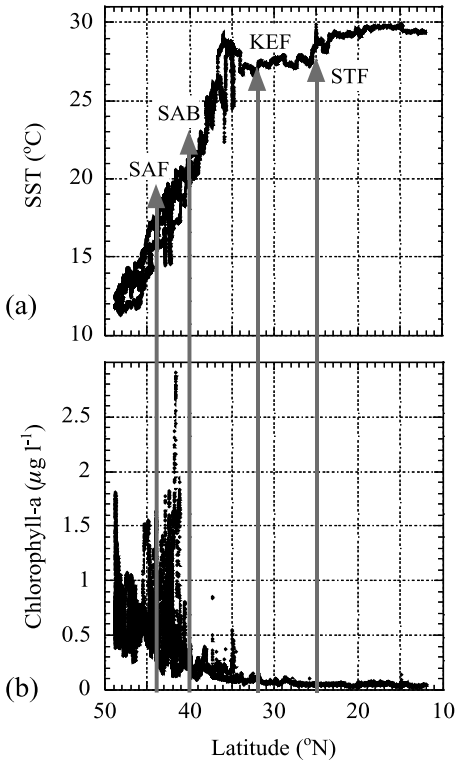

Figure 3. Latitudinal distributions of (a) SST and (b) chlorophyll-a concentration in surface seawater. Grey arrows show the locations of subarctic front (SAF), subarctic boundary (SAB), Kuroshio extension front (KEF), and subtropical front (STF).

16–20°C); (3) southern transition water (TW_S) between the subarctic boundary and the Kuroshio extension front in 32–40°N (approximately SST = 20–27°C); (4) northern subtropical water (ST_N) between the Kuroshio extension front and the subtropical front in 32–25°N (approximately with SST = 27–28°C); and (5) southern subtropical water (ST_S) to the south of the subtropical front in 25–12°N (approximately SST = 28–30°C). Warm water with SST = 28–29°C was found around 35°N 155°E within the TW_S water that came from the Kuroshio current.

[12] We found high concentrations of chlorophyll-a in SA surface seawater (average, 0.68 μg l^{-1}) and in TW_N water (average 0.56 μg l^{-1}). The average chlorophyll-a concentrations of TW_S, ST_N, and ST_S were 0.15 μg l^{-1}, 0.07 μg l^{-1}, and 0.05 μg l^{-1}, respectively. The biological production in the oligotrophic ST_N and ST_S waters was low compared to the waters of the other regions.

3.3. Latitudinal Distributions of pCH_3X and pHCFC-22 in Surface Seawater and the Marine Boundary Layer

[13] Latitudinal distributions of $p\mathrm{VOC}_{water}$ and $p\mathrm{VOC}_{air}$ are shown in Figure 4. The variation of pCH_3X_{air} during the cruise was much less than that of pCH_3X_{water}. The saturation anomaly of a VOC (S_{VOC}) is defined as:

$$S_{VOC} = (p\mathrm{VOC}_{water} - p\mathrm{VOC}_{air})/p\mathrm{VOC}_{air}, \quad (1)$$

where $p\mathrm{VOC}_{water}$ is the partial pressure in water and $p\mathrm{VOC}_{air}$ in air. Values for pVOC and S_{VOC} are summarized in Tables 1 and 2, respectively.

3.3.1. HCFC-22

[14] The average $p\mathrm{HCFC\text{-}22}_{air}$ of 203 pptv (1 σ = 9.0, n = 99) during the cruise was consistent with the summertime average (204 pptv) in 2008 at Cape Ochiishi (43°N, 145°E) in the northern part of Japan [*Yokouchi et al.*, 2009]. The $p\mathrm{HCFC\text{-}22}_{water}$ in SA, TW_N, TW_S, and ST_N waters were slightly higher than the average $p\mathrm{HCFC\text{-}22}_{air}$ of all the samples, whereas $p\mathrm{HCFC\text{-}22}_{water}$ in ST_S water was slightly below the average of $p\mathrm{HCFC\text{-}22}_{air}$. We found higher SHCFC-22 in the colder waters, ranging from −0.02 to 0.10 (Table 2). SST increased in SA water (+4°C $month^{-1}$) at 45°N, 155°E from July to August 2008 and at a faster rate than in ST_S water (+0.5°C $month^{-1}$) at 25°N, 155°E according to Japan Meteorological Agency (http://www.jma.go.jp/jma/index.html). The relatively high SHCFC-22 in SA water could be explained by the rapid decrease of solubility as a result of the rise in SST.

3.3.2. CH_3Cl

[15] The average $p\mathrm{CH_3Cl}_{air}$ of 583 pptv (1 σ = 47, n = 110) during the cruise was higher than the annual global average of 550 pptv [*WMO*, 2007]. On the whole, $p\mathrm{CH_3Cl}_{water}$ increased toward the south. For most of the SA water, $p\mathrm{CH_3Cl}_{water}$ was less than $p\mathrm{CH_3Cl}_{air}$, with an average SCH_3Cl of −0.07. In TW_N water, high levels of $p\mathrm{CH_3Cl}_{water}$ (up to 1313 pptv) were frequently observed. In TW_S water, there were high levels of $p\mathrm{CH_3Cl}_{water}$ (up to 1645 pptv) around 35°N 155°E in the warm Kuroshio water. In ST_S water, the $p\mathrm{CH_3Cl}_{water}$ maximum was present between 15°N and 20°N, where a SST maximum of up to 30°C could be seen (Figure 3b). The highest $p\mathrm{CH_3Cl}_{water}$ in ST_S (1893 pptv) was 1.6 times the previously reported highest value (1200 pptv) in the subtropical East Pacific [*Moore et al.*, 1996]. A higher (or lower) SCH_3X compared to SHCFC-22 suggests chemical or biological production (or loss) of CH_3X in surface seawater, because the saturation anomaly of long-lived HCFC-22 is mainly controlled by changes of temperature-dependent solubility in seawater and air-sea exchange. The supersaturation levels of CH_3Cl (SCH_3Cl = 0.48–1.6), which were higher than those of HCFC-22 (SHCFC-22 = −0.02 to 0.08) in TW_N, TW_S, ST_N, and ST_S waters, indicates net production of CH_3Cl in these waters. Similar levels of supersaturation (SCH_3Cl = 0.38) in surface seawater warmer than 12°C around 40°N in the northwest Atlantic in summer were attributed to net production of CH_3Cl [*MacDonald and Moore*, 2007]. In contrast, the slight undersaturation (SCH_3Cl = −0.07) in SA water suggests net loss of CH_3Cl in the surface seawater. Similar levels of undersaturation (SCH_3Cl = −0.03 to −0.15) have been found in the North Atlantic around 45–50°N in summer [*MacDonald and Moore*, 2007] and were attributed to bacterial degradation [*Tokarczyk et al.*, 2003a, 2003b].

3.3.3. CH_3Br

[16] The average $p\mathrm{CH_3Br}_{air}$ of 8.2 pptv (1 σ = 1.1, n = 110) during the cruise was consistent with the northern hemispheric average of 7.7 pptv in summer of 2008 [*Yvon-Lewis et al.*, 2009]. As with CH_3Cl, in SA water most $p\mathrm{CH_3Br}_{water}$ values were less than $p\mathrm{CH_3Br}_{air}$, with SCH_3Br = −0.12, and in TW_N water, high levels of $p\mathrm{CH_3Br}_{water}$ (up to 35 pptv) were frequently present, with

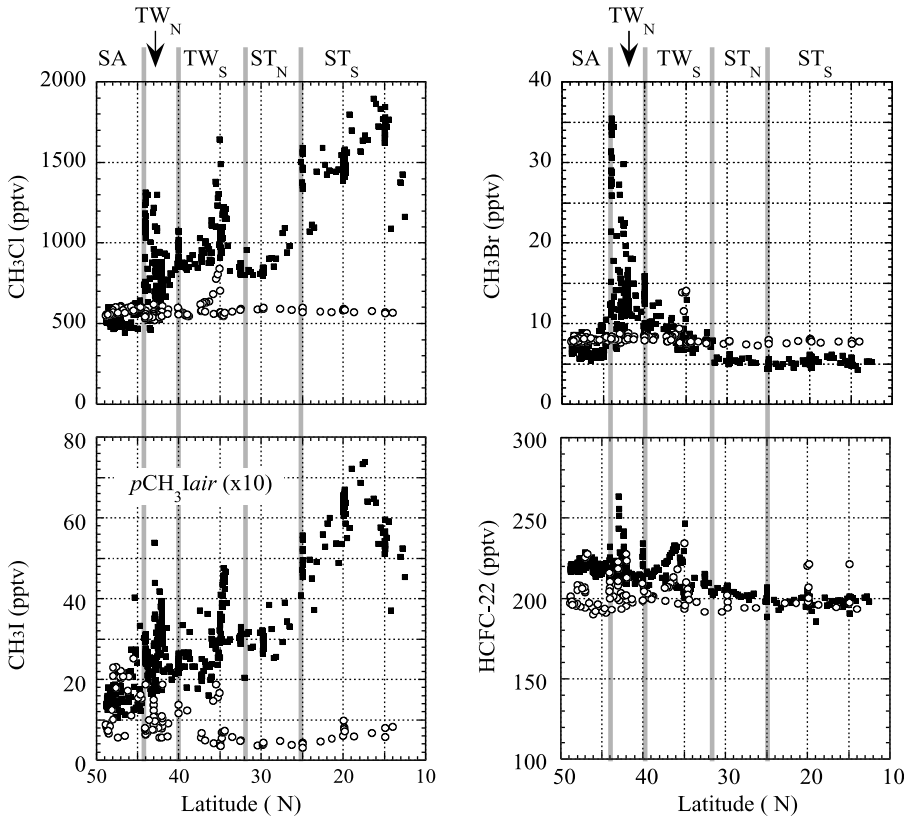

Figure 4. Latitudinal distributions of partial pressures (pptv) of CH_3X and HCFC-22 in surface seawater (squares) and the MBL (circles). SA, subarctic water; ST_N, northern subtropical water; and ST_S, southern subtropical water; TW_N, northern transition water; and TW_S, southern transition water. See section 3.2 for water mass details. The plots of pCH_3I_{air} were decoupled in the figure.

SCH_3Br = 0.95. In TW_S water, pCH_3Br_{water} gradually declined southward, from 10 pptv to 8 pptv, and dropped below pCH_3Br_{air} at 32°N near the Kuroshio extension front. In ST_N and ST_S waters, pCH_3Br_{water} remained below pCH_3Br_{air} with average SCH_3Br values of −0.27 and −0.33, respectively. The values of SCH_3Br in SA, ST_N and ST_S (−0.12, −0.27 and −0.33) were similar to those in polar and tropical waters of the Atlantic and Pacific Oceans (SCH_3Br = −0.15 to −0.36) from the cruises in spring/summer of 1998−1999 [*King et al.*, 2002]. SCH_3Br of 0.95 in TW_N was higher than the supersaturation (SCH_3Br = 0.5–0.6) observed in Atlantic Ocean water (41−42°N) in summer of 1998 [*King et al.*, 2000]. *Yvon-Lewis et al.* [2009] estimated the change of annual saturation state of CH_3Br in the global ocean, shifting from −0.12 in 1996 to −0.06 in 2007, owing to the decline of atmospheric CH_3Br level during the phaseout period since 1998. The saturation state of CH_3Br in our study area would have been affected by the decline of atmospheric CH_3Br level. However, we cannot analyze the interannual change of the saturation state in detail, because our measurements are limited to the NW Pacific from subarctic to subtropical in summer of 2008. More measurements covering the oceans where the saturation states of CH_3Br have been measured before the phaseout should be required to evaluate the interannual change of the saturation state.

Table 1. Ranges (Averages) of $pVOC_{air}$ and $pVOC_{water}$ in Different Water Masses[a]

	SA (44–49°N)	TW_N (40–44°N)	TW_S (32–40°N)	ST_N (25–32°N)	ST_S (12–25°N)	All (12–49°N)
CH_3Cl Water (pptv)	446–742 (537)	462–1313 (841)	801–1645 (1007)	798–1095 (871)	1072–1893 (1530)	446–1894 (959)
Air (pptv)	549–607 (579)	521–609 (559)	546–840 (603)	583–597 (590)	564–600 (578)	521–840 (583)
CH_3Br Water (pptv)	5.4–12 (7.1)	7.0–35 (16)	6.4–13 (8.4)	4.9–7.9 (5.5)	4.3–6.2 (5.2)	4.3–35 (9.8)
Air (pptv)	7.7–8.9 (8.1)	7.6–8.8 (8.2)	7.4–14 (8.7)	7.3–7.9 (7.6)	7.5–8.1 (7.8)	7.3–14 (8.2)
CH_3I Water (pptv)	11–40 (17)	16–54 (27)	16–48 (30)	25–39 (30)	37–74 (58)	11–74 (32)
Air (pptv)	0.56–2.5 (1.5)	0.56–1.9 (0.91)	0.35–1.9 (0.84)	0.36–0.48 (0.41)	0.30–0.98 (0.63)	0.30–2.5 (0.99)
HCFC-22 Water (pptv)	214–229 (220)	209–263 (220)	200–246 (212)	199–208 (204)	186–207 (199)	186–263 (214)
Air (pptv)	190–228 (200)	193–228 (204)	192–234 (204)	192–202 (196)	194–221 (204)	190–234 (203)

[a] $pVOC_{water}$ is the partial pressure in water and $pVOC_{air}$ in air. Abbreviations are as follows: SA, subarctic water; ST_N, northern subtropical water; ST_S, southern subtropical water; TW_N, northern transition water; and TW_S, southern transition water. See section 3.2 for water mass details. Here pptv = 1×10^{-12}. Values in parentheses represent averages.

Table 2. Averages of the Saturation Anomaly[a]

	SA (44–49°N)	TW_N (40–44°N)	TW_S (32–40°N)	ST_N (25–32°N)	ST_S (12–25°N)	All (12–49°N)
CH_3Cl	−0.07	0.50	0.67	0.48	1.6	0.64
CH_3Br	−0.12	0.95	−0.03	−0.27	−0.33	0.20
CH_3I	10	29	35	72	91	31
HCFC-22	0.10	0.08	0.04	0.04	−0.02	0.05

[a]Abbreviations are as follows: SA, subarctic water; ST_N, northern subtropical water; ST_S, southern subtropical water; TW_N, northern transition water; and TW_S, southern transition water. See section 3.2 for water mass details.

3.3.4. CH_3I

[17] The range of pCH_3I_{air} was 0.30–2.5 pptv (average 0.99 pptv, 1 σ = 0.57, n = 95) during the cruise and was consistent with the previously reported values of 0.5–2 pptv in the MBL over the NW Pacific in August–October when an annual maximum was found [*Yokouchi et al.*, 2001]. On the whole, pCH_3I_{water} increased toward the south. During the cruise, pCH_3I_{water} was much higher than pCH_3I_{air} with an average SCH_3I of 31, indicating net production of CH_3I in the surface seawater. As with CH_3Cl, high levels of pCH_3I_{water} were frequently observed in TW_N water and in the warm Kuroshio water at 35°N, 155°E. The pCH_3I_{water} maximum was between 15°N and 20°N. Previous studies have also reported higher values for pCH_3I_{water} in the mixed water and the subtropical water [*Schall et al.*, 1997; *Smythe-Wright et al.*, 2006]. The average pCH_3I_{water} (32 pptv) during the cruise was somewhat higher than the previously reported values for tropical water (average 25 pptv, range 11–44 pptv), central gyre water (average 21 pptv, range 6.2–49 pptv), and coastal water (average 15 pptv, range 2.9–32 pptv) of the Atlantic and Pacific Oceans observed during various seasons [*Butler et al.*, 2007].

3.4. Air-Sea Flux and Chloride Substitution

[18] In order to discuss production and loss of CH_3Xs in seawater, we estimated air-sea flux and chloride substitution of CH_3Xs in the mixed layer of the ocean along the ship's track along 155°E from 13°N to 44°N and 160°E from 40°N to 47°N at 1° intervals, where the CTD depth profiles were obtained. Air-sea flux of CH_3X (FCH_3X; nmol m^{-2} h^{-1}) were calculated by:

$$FCH_3X = -K \cdot (pCH_3X_{water} - pCH_3X_{air}) \cdot HCH_3X, \quad (2)$$

where K is the gas transfer velocity (cm s^{-1}), which depends on wind speed [*Wanninkhof*, 1992]. The average wind speed over the 2 weeks prior to sampling at each location was obtained from the meteorological analysis data of HYSPLIT (NOAA; http://www.ready.noaa.gov/ready/open/hysplit4.html) and used for the air-sea flux calculation. HCH_3X is the temperature-dependent Henry's law constant (mol l^{-1} atm^{-1}) obtained from *Moore* [2000] for CH_3Cl, *Wilhelm et al.* [1977] for CH_3Br, and *Hunter-Smith et al.* [1983] for CH_3I. Positive and negative values of air-sea flux mean air-to-sea influx and sea-to-air efflux, respectively.

[19] Molar concentrations (pmol l^{-1}) of CH_3X (CCH_3X) in seawater were calculated by:

$$CCH_3X = HCH_3X \cdot pCH_3X_{water}. \quad (3)$$

The loss rates of CH_3Br and CH_3I per unit volume (VCH_3Br and VCH_3I; pmol l^{-1} h^{-1}) via chloride substitution can be calculated by the following equations:

$$VCH_3Br = -kCH_3Br \cdot CCH_3Br \cdot [Cl^-] \quad (4)$$

$$VCH_3I = -kCH_3I \cdot CCH_3I \cdot [Cl^-], \quad (5)$$

where $[Cl^-]$ is the molar concentration of Cl^- (pmol l^{-1}) in seawater. The chloride substitution rate constants kCH_3Br

Table 3. Air-Sea Flux and Chloride Substitution Rate per Unit Area in the Mixed Layer of the Ocean Surface[a]

	Water Type						
	SA	TW_N	TW_S	ST_N	ST_S	Average	Global Average
Mixed layer depth (m)	15	18	17	21	38	25	
Wind speed (m s^{-1})	4.1	5.2	5.7	6.1	4.4	5.1	
SST (°C)	13.9	17.8	25.3	27.4	29.3	24.6	
			CH_3Cl (nmol m^{-2} h^{-1})				
Air-sea flux	+0.71	−4.1	−4.2	−4.1	−5.5	−4.2	−2.0 to −4.1[b]
ACH_3Cl	+0.05	+0.21	+0.32	+0.47	+1.7	0.75	
			CH_3Br (nmol m^{-2} h^{-1})				
Air-sea flux	+0.03	−0.20	−0.02	+0.05	+0.03	−0.02	+0.03 to +0.07[c]
ACH_3Br	−0.03	−0.15	−0.16	−0.16	−0.37	−0.22	
			CH_3I (nmol m^{-2} h^{-1})				
Air-sea flux	−0.15	−0.37	−0.39	−0.51	−0.41	−0.39	−0.5 to −1.4[d]
ACH_3I	−0.02	−0.07	−0.16	−0.31	−1.3	−0.53	

[a]Positive values indicate addition to the mixed layer (air-to-sea influx and chloride substitution production); negative values indicate removal from the mixed layer (sea-to-air efflux and chloride substitution loss). Abbreviations are as follows: SA, subarctic water; ST_N, northern subtropical water; ST_S, southern subtropical water; TW_N, northern transition water; and TW_S, southern transition water. See section 3.2 for water mass details.
[b]See *Khalil et al.* [1999], *Moore* [2000], and *Yoshida et al.* [2004].
[c]See *Lobert et al.* [1995], *Groszko and Moore* [1998], and *King et al.* [2002].
[d]See *Bell et al.* [2002] and *Butter et al.* [2007].

Table 4. Average Ranges of Different VOC Concentrations in Surface Seawater[a]

	SA (44–49°N)	TW_N (40–44°N)	TW_S (32–40°N)	ST_N (25–32°N)	ST_S (12–25°N)	All (12–49°N)
CH_3Cl (pmol l^{-1})	62–93 (74)	62–156 (97)	67–132 (86)	66–89 (72)	84–144 (117)	62–156 (93)
CH_3Br (pmol l^{-1})	1.3–2.8 (1.8)	1.7–7.5 (3.3)	0.92–2.5 (1.3)	0.72–1.2 (0.81)	0.59–0.85 (0.72)	0.59–7.5 (1.9)
CH_3I(pmol l^{-1})	3.6–12 (5.4)	4.3–15 (7.0)	2.9–7.9 (5.4)	4.4–6.7 (5.2)	5.9–12 (9.2)	2.9–15 (6.6)
HCFC-22 (pmol l^{-1})	9.2–12 (11)	7.4–12 (8.9)	5.4–8.1 (6.3)	5.5–5.8 (5.7)	4.8–5.5 (5.2)	4.8–12 (7.7)

[a] Abbreviations are as follows: SA, subarctic water; ST_N, northern subtropical water; ST_S, southern subtropical water; TW_N, northern transition water; and TW_S, southern transition water. See section 3.2 for water mass details.

and kCH_3I (l mol^{-1} s^{-1}) were obtained from *Elliott and Rowland* [1993] and *Jones and Carpenter* [2007], respectively, as:

$$kCH_3Br = \left(9.53 \times 10^{12}\right) \cdot \mathrm{Exp}(-12679/T) \quad (6)$$

$$kCH_3I = \left(3.66 \times 10^{13}\right) \cdot \mathrm{Exp}(-13317/T), \quad (7)$$

where T is seawater temperature (°C). Production rate of CH_3Cl per unit volume (VCH_3Cl; pmol l^{-1} h^{-1}) as a result of chloride substitution of CH_3Br and CH_3I can be calculated by the following equation:

$$VCH_3Cl = -(VCH_3Br + VCH_3I). \quad (8)$$

The chloride substitution (loss or production) rate of CH_3X per unit area (ACH_3X; nmol m^{-2} h^{-1}) in the mixed layer was defined by:

$$ACH_3X = VCH_3X \cdot z, \quad (9)$$

where z is the mixed layer depth (MLD; m), defined as the depth where the potential density has increased by 0.125 kg m^{-3} compared to that at the reference depth of 10 m. Positive and negative values of ACH_3X mean production and loss of CH_3X via chloride substitution in the mixed layer, respectively.

[20] The averages of air-sea flux and chloride substitution rate per unit area from this study are summarized in Table 3. In TW_N, TW_S, ST_N, and ST_S waters, the average sea-to-air efflux of CH_3Cl (4.1–5.5 nmol m^{-2} h^{-1}) was higher than the annual global oceanic mean efflux of 2.0−4.1 nmol m^{-2} h^{-1} [*Khalil et al.*, 1999; *Moore*, 2000; *Yoshida et al.*, 2004]. In these same waters of our study, the production of CH_3Cl via chloride substitution (0.21–1.7 nmol m^{-2} h^{-1}) compensated for 5–32% of the sea-to-air efflux.

[21] On average, the ocean surface in our study area was a weak source of CH_3Br, with an average sea-to-air efflux of 0.02 nmol m^{-2} h^{-1}, most of which was attributable to the strong efflux of 0.20 nmol m^{-2} h^{-1} in TW_N water. On annual global average, the ocean surface is estimated to be a net sink for CH_3Br, with a mean influx of 0.03–0.07 nmol m^{-2} h^{-1} [*Lobert et al.*, 1995; *Groszko and Moore*, 1998; *King et al.*, 2002]. The chloride substitution loss of CH_3Br (0.03 nmol m^{-2} h^{-1}) in SA water was comparable to the air-to-sea influx (0.03 nmol m^{-2} h^{-1}). In contrast, the chloride substitution loss in ST_N and ST_S waters (0.16–0.37 nmol m^{-2} h^{-1}) was 3–12 times the air-to-sea influx (0.03–0.05 nmol m^{-2} h^{-1}). This suggests that chloride substitution loss has largely contributed to the decline of CH_3Br levels to undersaturation in ST_N and ST_S waters.

[22] The average sea-to-air efflux of CH_3I (0.39 nmol m^{-2} h^{-1}) in our study area was a little smaller than the averaged global oceanic efflux of 0.50 nmol m^{-2} h^{-1} [*Bell et al.*, 2002]. The total of sea-to-air efflux and chloride substitution loss of CH_3I increased going southward from SA water (0.17 nmol m^{-2} h^{-1}) to ST_S water (1.7 nmol m^{-2} h^{-1}). This indicates that the net production of CH_3I in the subtropical water is much greater than in the subarctic water.

3.5. Relationships Between Seawater VOC Concentrations and SST

[23] Previous studies have given relationships between saturation anomalies for CH_3Cl and CH_3Br and SST. As for CH_3I, saturation anomaly is significantly affected by the change of pCH_3I_{air} (0.30–2.5 pptv). Production and loss of CH_3I in seawater are reflected in the change of CCH_3I rather than SCH_3I. To examine production and loss of CH_3X, we use the relationships between CVOC and SST. The averages and ranges of the CVOCs are listed in Table 4. The relationships between C_{VOC} and SST are shown in Figure 5.

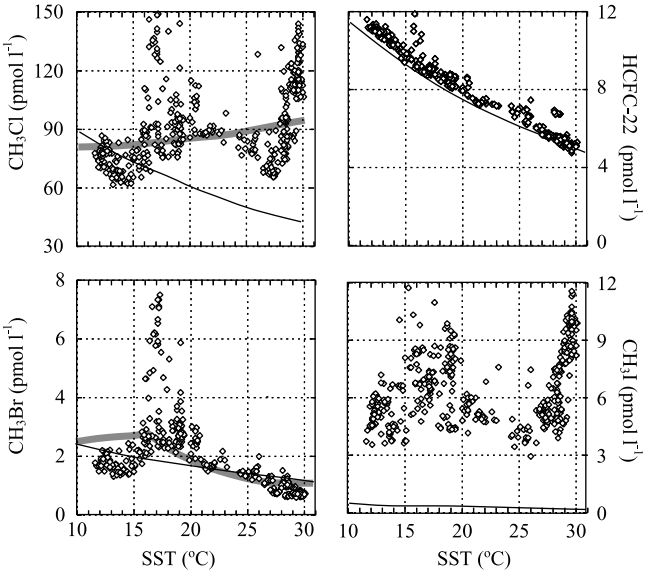

Figure 5. Relationship between VOC concentrations (CVOCs) and sea surface temperature (SST). The solid thin lines indicate the equilibrium concentrations with respect to the average partial pressures for pCH_3Cl_{air} (583 pptv), pCH_3Br_{air} (11 pptv), pCH_3I_{air} (0.99 pptv), and $pHCFC\text{-}22_{air}$ (203 pptv). The equilibrium concentrations were calculated by equation (3). Bold gray lines in the CH_3Cl and CH_3Br panels present empirical relationships on the basis of SCH_3Cl (%) = −24.1 + 0.159T^2 [*Khalil et al.*, 1999] and SCH_3Br (%) = 0.17065T^2 + 1.91413T − 33.85496 for T < 16°C, and SCH_3Br (%) = 0.48994T^2 − 26.70125T + 349.14043 for T > 16°C [*King et al.*, 2002].

The concentrations of individual VOCs in seawater at equilibrium with the respective average $p\mathrm{VOC}_{air}$ were calculated by equation (3) and shown as thin solid lines in Figure 5. Bold gray lines in the CH_3Cl and CH_3Br panels present empirical relationships on the basis of: $S\mathrm{CH_3Cl}\ (\%) = -24.1 + 0.159T^2$ [*Khalil et al.*, 1999] and $S\mathrm{CH_3Br}\ (\%) = 0.17065T^2 + 1.91413T - 33.85496$ for $T < 16°C$; $S\mathrm{CH_3Br}\ (\%) = 0.48994T^2 - 26.70125T + 349.14043$ for $T > 16°C$) [*King et al.*, 2002]. $S\mathrm{CH_3Cl}$ and $S\mathrm{CH_3Br}$ are the saturation anomalies for CH_3Cl and CH_3Br, respectively, and T = SST (°C). Saturation anomalies of the empirical equations were converted to CVOCs (pmol l^{-1}) by equations (1) and (3) using a respective constant $p\mathrm{VOC}_{air}$ value. The average $p\mathrm{CH_3Cl}_{air}$ (583 pptv) during this cruise was used to convert the empirical equation of $S\mathrm{CH_3Cl}$ by *Khalil et al.* [1999]. The atmospheric CH_3Br level has been declined during the phaseout period owing to the Montreal Protocol [*Yokouchi et al.*, 2002]. The average $p\mathrm{CH_3Br}_{air}$ of 11 pptv measured during the prephaseout period was used to convert the empirical equation of $S\mathrm{CH_3Br}$ by *King et al.* [2002].

3.5.1. CH_3Cl Versus SST

[24] The scatterplot of $C\mathrm{CH_3Cl}$ versus SST has high values and much scatter both in the SST range from 16 to 20°C (TW_N water) and from 27 to 30°C (ST_N and ST_S waters) (Figure 5). Between SSTs of 16 and 20°C, where high concentrations of chlorophyll-a were observed, the average $C\mathrm{CH_3Cl}$ (97 pmol l^{-1}) and the maximum $C\mathrm{CH_3Cl}$ (156 pmol l^{-1}) are 1.1 and 1.8 times that of the average value (84 pmol l^{-1}) calculated from the empirical equation in the same SST range. As direct evidence for the production of CH_3Cl from phytoplankton has been reported [e.g., *Scarratt and Moore*, 1996, 1998], we considered that the high $C\mathrm{CH_3Cl}$ in TW_N was due to enhanced production by phytoplankton.

[25] In the SST range 27–30°C, where the chlorophyll-a concentrations were low, $C\mathrm{CH_3Cl}$ sharply increased from 66 pmol l^{-1} to 144 pmol l^{-1} with the SST rise. The maximum $C\mathrm{CH_3Cl}$ (144 pmol l^{-1}) observed at SST = 30°C is 1.5 times the value of 95 pmol l^{-1} calculated with the empirical equation at the same SST [*Khalil et al.*, 1999]. Chloride substitutions of CH_3Br and CH_3I has been regarded as an important abiotic process of CH_3Cl production in seawater [*Elliott and Rowland*, 1993; *Jones and Carpenter*, 2007], and was estimated to account for ~40–75% of the global oceanic source of CH_3Cl [*Moore et al.*, 1996]. The chloride substitution production of CH_3Cl (1.7 nmol m^{-2} h^{-1}) in ST_S water is estimated to compensate for 31% of the sea-to-air efflux (5.5 nmol m^{-2} h^{-1}), even though the determination of MLD could directly influence the flux calculation as expressed in equation (9).

[26] This result implies that there is still a large source of CH_3Cl in the surface ST_S water other than chloride substitution production; for example, photochemical reactions involving colored dissolved organic matter (CDOM) in seawater [*Moore*, 2008]. *Moore* [2008] reported that terrestrially derived humic-like CDOM in a chloride solution yielded CH_3Cl through a photochemical process. He also found that high-molecular-weight (HMW) DOM of 1 kDa to 0.2 μm in size, which had been extracted from subsurface water (at 600 m depth) in the subtropical North Pacific, showed some ability to enhance photochemical production of CH_3Cl, while HMW-DOM from surface seawater did not.

[27] It should be mentioned that *Moore* [2008] found that surface seawater with no HMW-DOM supplement produced CH_3Cl at a rate of ~5 pmol l^{-1} h^{-1} after irradiation by a solar simulator with wavelengths between 300 and 800 nm. This result implies the existence of certain kind of DOM, other than HMW-DOM, involving the photochemical production of CH_3Cl in seawater, that is, low-molecular-weight DOM (LMW-DOM) < 1 kDa in size which accounts for a large fraction (65–80%) of the bulk DOM from surface to deep waters [*Ogawa and Tanoue*, 2003]. Humic-like DOM would be necessary for the photochemical production of CH_3Cl as referred above. In the surface layer of the open ocean, in situ production of humic-like fluorescent DOM (FDOM; excitation maximum at $\lambda = 320$ nm), which occurs simultaneously with photochemical degradation, was ascertained by field observation [*Yamashita and Tanoue*, 2008]. We suggest that it is possible that humic-like LMW-FDOM, which can be produced in the surface of the open ocean, is capable of producing CH_3Cl through photochemical reactions, and that the photochemical production rate of CH_3Cl by LMW-FDOM at the surface (probably 5 pmol l^{-1} h^{-1} in maximum) is considerably higher than the chloride substitution production rate of 0.04 pmol l^{-1} h^{-1} observed in ST_S water of the NW Pacific. If LMW-FDOM is biologically produced by temperature-dependent enzymatic reactions in seawater, the higher SST could lead the higher photochemical production rate of CH_3Cl. Photochemical production as well as chloride substitution would contribute to production of CH_3Cl in the surface of subtropical waters.

3.5.2. CH_3Br Versus SST

[28] In the SST range 16–20°C (TW_N water), we found a significant peak of $C\mathrm{CH_3Br}$ (up to 7.5 pmol l^{-1}), and the average $C\mathrm{CH_3Br}$ of 3.3 pmol l^{-1} is close to the value calculated from the empirical equation (2.9 pmol l^{-1}) for the same SST range during the prephaseout period. The average $C\mathrm{CH_3Br}$ of 1.8 pmol l^{-1} within SST range 11–16°C and 0.72 pmol l^{-1} within 28–30°C are lower than the values of 3.3 pmol l^{-1} and 1.3 pmol l^{-1} calculated from the empirical equation for the same SST ranges, respectively.

[29] We compared $C\mathrm{CH_3Cl}$ and $C\mathrm{CH_3Br}$ in SA and TW_N waters (Figure 6a). We found strong correlations between $C\mathrm{CH_3Br}$ and $C\mathrm{CH_3Cl}$ in SA water ($r^2 = 0.78$) and in TW_N water ($r^2 = 0.85$). A strong correlation ($r^2 = 0.89$) between concentrations of these two compounds has been also found in subarctic northwest Atlantic waters cooler than 23°C, and attributed to similarities in biological production and/or loss of these gases [*MacDonald and Moore*, 2007]. There is no correlation between $C\mathrm{CH_3Cl}$ and $C\mathrm{CH_3Br}$ ($r^2 = 0.15$) in ST_N and ST_S waters where the biological production was low based on chlorophyll-a concentration data. It is clear that production and loss processes of CH_3Br in ST waters are different from those of CH_3Cl.

3.5.3. CH_3I Versus SST

[30] As with CH_3Cl, the plot of $C\mathrm{CH_3I}$ versus SST had concentration peaks both for SST = 16–20°C (up to 15 pmol l^{-1}) and for SST = 27–30°C (up to 12 pmol l^{-1}). Similar substantial increases of CH_3I (up to 9.7 pmol l^{-1}) have been measured in the mixed water region of the Atlantic (40°S), where substantially higher chlorophyll-a concentrations have been also detected [*Schall et al.*, 1997]. There is direct evidence for the production of CH_3I from phyto-

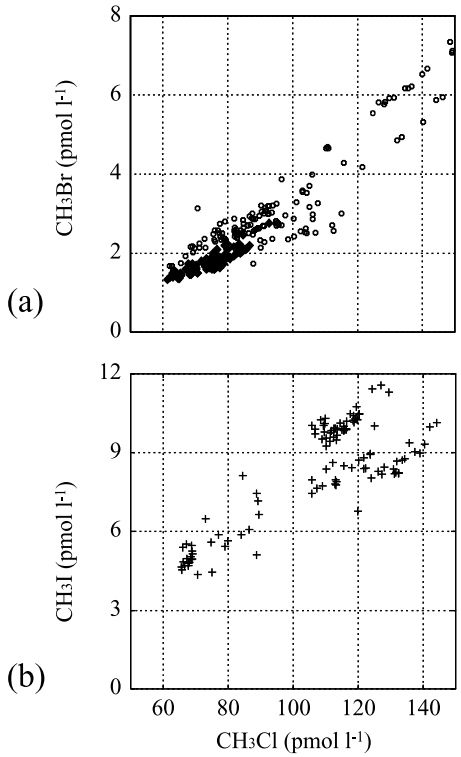

Figure 6. Scatterplots of methyl halide concentrations. (a) CCH_3Cl versus CCH_3Br in SA (subarctic) water (diamonds) and TW_N (northern transition) water (circles). (b) CCH_3Cl versus CCH_3I in ST_N (northern subtropical water) and ST_S (southern subtropical water) (pluses).

plankton [e.g., *Manley and dela Cuesta*, 1997; *Scarratt and Moore*, 1998]. We considered that high CCH_3I in SST range 16–20°C (TW_N water) was due to enhanced production by phytoplankton. For SST = 27–30°C (ST_N and ST_S waters), we found that CCH_3I sharply increased from 4.4 pmol l^{-1} to 12 pmol l^{-1} with the increase in SST. Similar significant increases ranging from 6.0 to 12 pmol l^{-1} have been found in summer in the subtropical South Atlantic (19°S) [*Happell and Wallace*, 1996].

[31] The significant increase of CCH_3I with SST rise in ST_N and ST_S waters could be due to photochemical production of CH_3I for the following reasons. *Moore and Zafiriou* [1994] proposed for CH_3I production a radical recombination mechanism of methyl radicals formed from the photolysis of humic materials with I radical formed from the photochemical oxidation of I^-. Dissolved I^- concentrations in oligotrophic subtropical waters are much higher than those in nutrient rich, subpolar and polar waters, because IO_3^- would be reduced to I^- in the absence of NO_3^- by enzymatic reaction [*Campos et al.*, 1999]. *Chuck et al.* [2005] also suggested that photochemical production of CH_3I is associated with nitrate reductase activity which could reduce IO_3^- . In general, enzymatic reactions are highly dependent on temperature. Therefore, the higher SST in subtropical water would lead to a higher photochemical production rate of CH_3I. The averaged photochemical production rate of CH_3I within the mixed layer of tropical seawater (MLD = 30 m) is estimated to be 1 nmol m^{-2} h^{-1} [*Richter and Wallace*, 2004], which is close to the total of sea-to-air efflux and chloride substitution loss (1.7 nmol m^{-1} h^{-1}) from our results in ST_S water.

[32] Other than photochemical production, the importance of biological production of CH_3I by *Prochlorococcus*, a genus of cyanobacteria that predominates in subtropical waters, was suggested by *Smythe-Wright et al.* [2006]. Although *Prochlorococcus* would directly produce CH_3I, it may also contribute to the biological reduction of IO_3^- to I^- similar to *Synechococcus* (a genus of cyanobacteria) [*Wong et al.*, 2002].

[33] *Wang et al.* [2009] pointed out two reasons why photochemical reactions can account for the positive correlation (r^2 = 0.37) that they observed in the North Atlantic (37–59°N) between CH_3I concentration and water temperature. First, higher temperature could promote biological CDOM formation, and second, photochemical reaction rate could be positively influenced by temperature. We supposed that higher SST and stronger light intensity in subtropical waters have promoted CH_3I production through photochemical pathway and biological pathways by direct emission of CH_3I from *Prochlorococcus* and/or by formations of

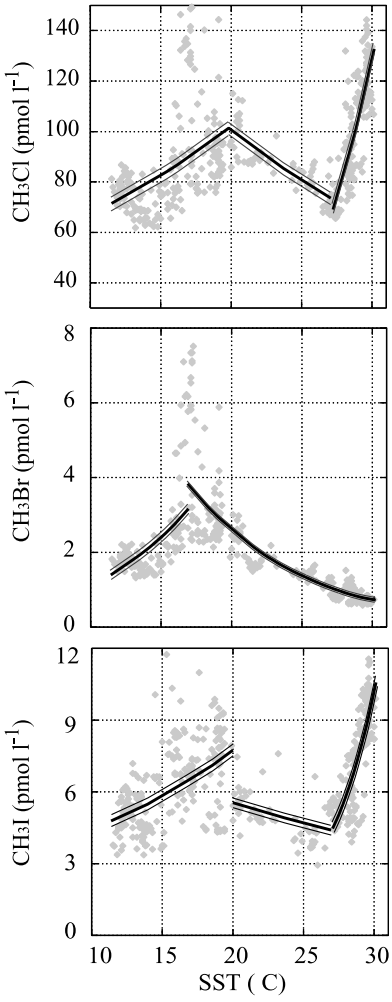

Figure 7. Empirical regression curves (bold solid lines) of methyl halide concentrations (CCH_3X) versus sea surface temperature (SST) with 95% confidence limits (gray lines). The equation parameters are in Table 5.

Table 5. Empirical Regression Formulas of Methyl Halides Concentrations in Surface Seawater as a Function of Sea Surface Temperature[a]

Methyl Halides (pmol l^{-1})	Formula	SST Range	r^2
CCH_3Cl	43.9·exp(0.0420·T)	11–20°C	0.20
	244·exp(−0.0443·T)	20–27°C	0.48
	0.147·exp(0.226·T)	27–30°C	0.69
CCH_3Br	0.27·exp(0.144·T)	11–17°C	0.43
	34.2·exp(−0.129·T)	17–30°C	0.74
CCH_3I	2.5·exp(0.0565·T)	11–20°C	0.19
	11·exp(−0.0346·T)	20–27°C	0.16
	0.0018·exp(0.288·T)	27–30°C	0.66

[a]SST, sea surface temperature. T = SST (°C). Here r^2 values are the correlations between the observed values and the calculated values from the regression formulas.

intermediates of photochemical reactions such as I^- and LMW-FDOM as a source of methyl radical. Furthermore, high correlation between CCH_3I and CCH_3Cl ($r^2 = 0.67$) in ST_N and ST_S waters (Figure 6b) implies a similarity in the production pathways of the 2 methyl halides.

3.6. Regression Analysis of Methyl Halide Concentrations

[34] Empirical regression curves of CH_3X concentrations are expressed as exponential functions of SST (Figure 7) and their formulas are listed in Table 5. As with the CH_3Cl and CH_3I concentration data presented above, the regression formulas are divided into 3 SST ranges of 11–20°C (SA and TW_N waters), 20–27°C (TW_S water), and 27–30°C (ST_N and ST_S waters). The CH_3Br regression formula is split at SST = 17°C, where the peak CCH_3Br was found in TW_N water. *Tokarczyk and Moore* [2006] point out that the saturation anomaly of CH_3Br in surface seawater cannot be predicted from the temperature data only in temperate areas with high biological activity where production and degradation processes of CH_3Br are likely to be more dynamic than SST change. Further research on the CH_3X distributions in various ocean waters for all seasons is needed for the precise estimation of global distributions of CH_3X and their oceanic air-sea flux.

4. Summary

[35] The partial pressures of CH_3X (X = Cl, Br, and I) in the surface seawater of the NW Pacific from subarctic to subtropical regions were found to vary spatially. In the northern transition water (mixed water region), which had high biological activity, high levels for the 3 CH_3X were frequently observed because phytoplankton could have contributed to their production. In the subtropical water, which had very low biological production, the latitudinal distributions of pCH_3Cl_{water} and pCH_3I_{water} had a peak between 15°N and 20°N where high SST values (up to 30°C) were observed. We found that CCH_3Cl and CCH_3I sharply increased with an SST rise in the subtropical water. We propose that photochemical production of CH_3I and CH_3Cl largely contributed to their enrichment in the surface of subtropical water. This may be the result of temperature-dependent enzymatic reactions producing intermediates of photochemical reactions such as LMW-FDOM and I^-.

[36] We calculated empirical regression formulas for CH_3X concentrations in surface seawater as exponential functions of SST. Regression formulas of CH_3Cl and CH_3I were divided into 3 SST ranges corresponding to the oceanic frontal boundaries. The regression formula for CH_3Br was split at SST = 17°C. Further research on CH_3X measurements in all seasons for various water types is needed for precise estimations of the global distributions of CH_3X and their air-sea flux.

[37] **Acknowledgments.** We would like to thank the chief scientists, captain, and crews of *Hakuho-maru* (cruise KH-08-2). We would also like to thank J. Nishioka and T. Yoshimura for the chlorophyll-a data. This research has been supported by the Grant-in-Aid for Scientific Research in priority areas Western Pacific Air-Sea Interaction Study under grant 18067012. This research is a contribution to the Surface Ocean Lower Atmosphere Study Core Project of the International Geosphere-Biosphere Programme.

References

Amachi, S., Y. Kamagata, T. Kanagawa, and Y. Muramatsu (2001), Bacteria mediate methylation of iodine in marine and terrestrial environments, *Appl. Environ. Microbiol.*, *67*, 2718–2722, doi:10.1128/AEM.67.6.2718-2722.2001.

Anbar, A. D., Y. L. Yung, and F. P. Chavez (1996), Methyl bromide: Ocean sources, ocean sinks, and climate sensitivity, *Global Biogeochem. Cycles*, *10*, 175–190, doi:10.1029/95GB02743.

Bell, N., L. Hsu, D. J. Jacob, M. G. Schultz, D. R. Blake, J. H. Butler, D. B. King, J. M. Lobert, and E. Maier-Reimer (2002), Methyl iodide: Atmospheric budget and use as a tracer of marine convection in global models, *J. Geophys. Res.*, *107*(D17), 4340, doi:10.1029/2001JD001151.

Butler, J. H., D. B. King, J. M. Lobert, S. A. Montzka, S. A. Yvon-Lewis, B. D. Hall, N. J. Warwick, D. J. Mondeel, M. Aydin, and J. W. Elkins (2007), Oceanic distributions and emissions of short-lived halocarbons, *Global Biogeochem. Cycles*, *21*, GB1023, doi:10.1029/2006GB002732.

Campos, M. L. A. M., R. Sanders, and T. Jickells (1999), The dissolved iodate and iodide distribution in the South Atlantic from the Weddell Sea to Brazil, *Mar. Chem.*, *65*, 167–175, doi:10.1016/S0304-4203(98)00094-2.

Chameides, W. L., and D. D. Davis (1980), Iodine: Its possible role in tropospheric photochemistry, *J. Geophys. Res.*, *85*, 7383–7398, doi:10.1029/JC085iC12p07383.

Chuck, A. L., S. M. Turner, and P. S. Liss (2005), Oceanic distributions and air-sea fluxes of biogenic halocarbons in the open ocean, *J. Geophys. Res.*, *110*, C10022, doi:10.1029/2004JC002741.

Elliott, S., and F. S. Rowland (1993), Nucleophilic-substitution rates and solubilities for methyl halides in seawater, *Geophys. Res. Lett.*, *20*, 1043–1046, doi:10.1029/93GL01081.

Giese, B., F. Laturnus, F. C. Adams, and C. Wiencke (1999), Release of volatile iodinated C-1-C-4 hydrocarbons by marine macroalgae from various climate zones, *Environ. Sci. Technol.*, *33*, 2432–2439, doi:10.1021/es980731n.

Groszko, W., and R. M. Moore (1998), Ocean-atmosphere exchange of methyl bromide: NW Atlantic and Pacific Ocean studies, *J. Geophys. Res.*, *103*, 16,737–16,741, doi:10.1029/98JD00111.

Happell, J. D., and D. W. R. Wallace (1996), Methyl iodide in the Greenland/Norwegian Seas and the tropical Atlantic Ocean: Evidence for photochemical production, *Geophys. Res. Lett.*, *23*, 2105–2108, doi:10.1029/96GL01764.

Hunter-Smith, R. J., P. W. Balls, and P. S. Liss (1983), Henry's law constants and the air-sea exchange of various low molecular weight halocarbon gases, *Tellus, Ser. B*, *35*, 170–176, doi:10.1111/j.1600-0889.1983.tb00021.x.

Jones, C. E., and L. J. Carpenter (2007), Chemical destruction of CH_3I, C_2H_5I, 1-C_3H_7I, and 2-C_3H_7I in saltwater, *Geophys. Res. Lett.*, *34*, L13804, doi:10.1029/2007GL029775.

Khalil, M. A. K., R. M. Moore, D. B. Harper, J. M. Lobert, D. J. Erickson, V. Koropalov, W. T. Sturges, and W. C. Keene (1999), Natural emissions of chlorine-containing gases: Reactive Chlorine Emissions Inventory, *J. Geophys. Res.*, *104*, 8333–8346, doi:10.1029/1998JD100079.

King, D. B., J. H. Butler, S. A. Montzka, S. A. Yvon-Lewis, and J. W. Elkins (2000), Implications of methyl bromide supersaturations in the temperate North Atlantic Ocean, *J. Geophys. Res.*, *105*, 19,763–19,769, doi:10.1029/2000JD900251.

King, D. B., J. H. Butler, S. A. Yvon-Lewis, and S. A. Cotton (2002), Predicting oceanic methyl bromide saturation from SST, *Geophys. Res. Lett.*, *29*(24), 2199, doi:10.1029/2002GL016091.

Lobert, J. M., J. H. Butler, S. A. Montzka, L. S. Geller, R. C. Myers, and J. W. Elkins (1995), A net sink for atmospheric CH_3Br in the east Pacific Ocean, *Science*, *267*, 1002–1005, doi:10.1126/science.267.5200.1002.

MacDonald, S., and R. M. Moore (2007), Seasonal and spatial variations in methyl chloride in NW Atlantic waters, *J. Geophys. Res.*, *112*, C05028, doi:10.1029/2006JC003812.

Manley, S. L. (1992), Laboratory production of bromoform, methylene bromide, and methyl-iodide by macroalgae and distribution in nearshore Southern California waters, *Limnol. Oceanogr.*, *37*, 1652–1659.

Manley, S. L., and M. N. Dastoor (1987), Methyl halide (CH_3X) production from the giant kelp, macrocystis, and estimates of global CH_3X production by kelp, *Limnol. Oceanogr.*, *32*, 709–715.

Manley, S. L., and J. L. delaCuesta (1997), Methyl iodide production from marine phytoplankton cultures, *Limnol. Oceanogr.*, *42*, 142–147.

Moore, R. M. (2000), The solubility of a suite of low molecular weight organochlorine compounds in seawater and implications for estimating the marine source of methyl chloride to the atmosphere, *Chemosphere*, *2*, 95–99.

Moore, R. M. (2008), A photochemical source of methyl chloride in saline waters, *Environ. Sci. Technol.*, *42*, 1933–1937, doi:10.1021/es071920l.

Moore, R. M., and O. C. Zafiriou (1994), Photochemical production of methyl iodide in seawater, *J. Geophys. Res.*, *99*, 16,415–16,420, doi:10.1029/94JD00786.

Moore, R. M., W. Groszko, and S. J. Niven (1996), Ocean-atmosphere exchange of methyl chloride: Results from NW Atlantic and Pacific Ocean studies, *J. Geophys. Res.*, *101*, 28,529–28,538, doi:10.1029/96JC02915.

Ogawa, H., and E. Tanoue (2003), Dissolved organic matter in oceanic waters, *J. Oceanogr.*, *59*, 129–147, doi:10.1023/A:1025528919771.

Ooki, A., and Y. Yokouchi (2008), Development of a silicone membrane tube equilibrator for measuring partial pressures of volatile organic compounds in natural water, *Environ. Sci. Technol.*, *42*, 5706–5711, doi:10.1021/es800912j.

Richter, U., and D. W. R. Wallace (2004), Production of methyl iodide in the tropical Atlantic Ocean, *Geophys. Res. Lett.*, *31*, L23S03, doi:10.1029/2004GL020779.

Scarratt, M. G., and R. M. Moore (1996), Production of methyl chloride and methyl bromide in laboratory cultures of marine phytoplankton, *Mar. Chem.*, *54*, 263–272, doi:10.1016/0304-4203(96)00036-9.

Scarratt, M. G., and R. M. Moore (1998), Production of methyl bromide and methyl chloride in laboratory cultures of marine phytoplankton II, *Mar. Chem.*, *59*, 311–320, doi:10.1016/S0304-4203(97)00092-3.

Schall, C., K. G. Heumann, and G. O. Kirst (1997), Biogenic volatile organoiodine and organobromine hydro carbons in the Atlantic Ocean from 42 degrees N to 72 degrees S, *Fresenius J. Anal. Chem.*, *359*, 298–305, doi:10.1007/s002160050577.

Smythe-Wright, D., S. M. Boswell, P. Breithaupt, R. D. Davidson, C. H. Dimmer, and L. B. E. Diaz (2006), Methyl iodide production in the ocean: Implications for climate change, *Global Biogeochem. Cycles*, *20*, GB3003, doi:10.1029/2005GB002642.

Solomon, S., R. R. Garcia, and A. R. Ravishankara (1994), On the role of iodine in ozone depletion, *J. Geophys. Res.*, *99*, 20,491–20,499, doi:10.1029/94JD02028.

Tokarczyk, R., and R. M. Moore (2006), A seasonal study of methyl bromide concentrations in the North Atlantic (35°–60°N), *J. Geophys. Res.*, *111*, D08304, doi:10.1029/2005JD006487.

Tokarczyk, R., K. D. Goodwin, and E. S. Saltzman (2003a), Methyl chloride and methyl bromide degradation in the Southern Ocean, *Geophys. Res. Lett.*, *30*(15), 1808, doi:10.1029/2003GL017459.

Tokarczyk, R., E. S. Saltzman, R. M. Moore, and S. A. Yvon-Lewis (2003b), Biological degradation of methyl chloride in coastal seawater, *Global Biogeochem. Cycles*, *17*(2), 1057, doi:10.1029/2002GB001949.

Tsuda, A., H. Sugisaki, T. Ishimaru, T. Saino, and T. Sato (1993), White-noise like distribution of an oceanic copepod *Neocalanus cristatus* in the subarctic Pacific, *Mar. Ecol. Prog. Ser.*, *97*, 39–46, doi:10.3354/meps097039.

Wang, L., R. M. Moore, and J. J. Cullen (2009), Methyl iodide in the NW Atlantic: Spatial and seasonal variation, *J. Geophys. Res.*, *114*, C07007, doi:10.1029/2007JC004626.

Wanninkhof, R. (1992), Relationship between wind-speed and gas-exchange over the ocean, *J. Geophys. Res.*, *97*, 7373–7382, doi:10.1029/92JC00188.

Welschmeyer, N. A. (1994), Fluorometric analysis of chlorophyll-a in the presence of chlorophyll-b and phaeopigments, *Limnol. Oceanogr.*, *39*, 1985–1992, doi:10.4319/lo.1994.39.8.1985.

Wilhelm, E., R. Battino, and R. J. Wilcock (1977), Low-pressure solubility of gases in liquid water, *Chem. Rev.*, *77*, 219–262, doi:10.1021/cr60306a003.

Wong, G. T. F., A. U. Piumsomboon, and W. M. Dunstan (2002), The transformation of iodate to iodide in marine phytoplankton cultures, *Mar. Ecol. Prog. Ser.*, *237*, 27–39, doi:10.3354/meps237027.

World Meteorological Organization (WMO) (2007), Scientific Assessment of Ozone Depletion: 2006, *Global Res. Monit. Proj. Rep.*, *50*, Geneva.

Yamashita, Y., and E. Tanoue (2008), Production of bio-refractory fluorescent dissolved organic matter in the ocean interior, *Nat. Geosci.*, *1*, 579–582, doi:10.1038/ngeo279.

Yasuda, I. (2003), Hydrographic structure and variability in the Kuroshio-Oyashio transition area, *J. Oceanogr.*, *59*, 389–402, doi:10.1023/A:1025580313836.

Yokouchi, Y., Y. Nojiri, L. A. Barrie, D. Toom-Sauntry, and Y. Fujinuma (2001), Atmospheric methyl iodide: High correlation with surface seawater temperature and its implications on the sea-to-air flux, *J. Geophys. Res.*, *106*, 12,661–12,668, doi:10.1029/2001JD900083.

Yokouchi, Y., D. Toon-Sauntry, K. Yazawa, T. Inagaki, and T. Tamaru (2002), Recent decline of methyl bromide in the troposphere, *Atmos. Environ.*, *36*, 4985–4989, doi:10.1016/S1352-2310(02)00650-7.

Yokouchi, Y., S. Taguchi, T. Saito, Y. Tohjima, H. Tanimoto, and H. Mukai (2006), High frequency measurements of HFCs at a remote site in East Asia and their implications for Chinese emissions, *Geophys. Res. Lett.*, *33*, L21814, doi:10.1029/2006GL026403.

Yokouchi, Y., et al. (2008), Global distribution and seasonal concentration change of methyl iodide in the atmosphere, *J. Geophys. Res.*, *113*, D18311, doi:10.1029/2008JD009861.

Yokouchi, Y., T. Saito, H. Mukai, T. Shirai, and S. Sugata (2009), Observational study of halocarbon greenhouse gases to infer changes in emissions in East Asia, interim report, Global Environ. Res. Coord. Syst., Minist. of the Environ. Jpn., Tokyo.

Yoshida, Y., Y. Wang, T. Zeng, and R. Yantosca (2004), A three-dimensional global model study of atmospheric methyl chloride budget and distributions, *J. Geophys. Res.*, *109*, D24309, doi:10.1029/2004JD004951.

Yvon-Lewis, S. A., E. S. Saltzman, and S. A. Montzka (2009), Recent trends in atmospheric methyl bromide: Analysis of post-Montreal Protocol variability, *Atmos. Chem. Phys.*, *9*, 5963–5974, doi:10.5194/acp-9-5963-2009.

S. Itoh and A. Tsuda, Atmosphere and Ocean Research Institute, University of Tokyo, Chiba 277-8568, Japan.

S. Kameyama, A. Ooki, and Y. Yokouchi, National Institute for Environmental Studies, 16-2 Onogawa, Tsukubu, Ibaraki 305-8506, Japan. (ooki.atsushi@nies.go.jp)

A. Okubo and S. Takeda, Graduate School of Agricultural and Life Sciences, University of Tokyo, Tokyo 113-8657, Japan.

T. Suga, Department of Geophysics, Graduate School of Science, Tohoku University, Miyagi 980-8578, Japan.

H. Tazoe, College of Humanities and Sciences, Nihon University, Tokyo 156-8550, Japan.